

Hopping transport in hostile reaction-diffusion systems

Andrew R. Missel* and Karin A. Dahmen†

Physics Department, University of Illinois at Urbana-Champaign, Urbana, Illinois 61801, USA

(Received 24 August 2008; revised manuscript received 13 January 2009; published 23 February 2009)

We investigate transport in a disordered reaction-diffusion model consisting of particles which are allowed to diffuse, compete with one another ($2A \rightarrow A$), give birth in small areas called “oases” ($A \rightarrow 2A$), and die in the “desert” outside the oases ($A \rightarrow 0$). This model has previously been used to study bacterial populations in the laboratory and is related to a model of plankton populations in the oceans. We first consider the nature of transport between two oases: In the limit of high growth rate, this is effectively a first passage process, and we are able to determine the first passage time probability density function in the limit of large oasis separation. This result is then used along with the theory of hopping conduction in doped semiconductors to estimate the time taken by a population to cross a large system.

DOI: [10.1103/PhysRevE.79.021126](https://doi.org/10.1103/PhysRevE.79.021126)

PACS number(s): 64.60.ah, 82.40.Ck, 72.20.Ee

I. INTRODUCTION

A. Disorder in reaction-diffusion models

Reaction-diffusion (RD) models have proven to be very useful tools for the study of chemical [1], biological [2–7], and ecological [8,9] systems. RD models typically consist of a set of particles which are allowed to diffuse and interact with one another and their environment in prescribed ways. By varying the types of allowed reactions, number of types of particles, and reaction rates, one can obtain a wide variety of behavior. Much work has been done to examine the phase transition between active (population survives as $t \rightarrow \infty$) and absorbing (population dies as $t \rightarrow \infty$) states [10–14] and to determine the nature of propagating fronts [15–18].

Typically, RD models are governed by a microscopic master equation [19] which describes the probability flow into and out of the microstates of the system. This master equation is not solvable for all but the most simple models, and thus various approximation techniques—Langevin equations, for example—are usually used. There does exist a systematic expansion of the master equation [19], the lowest order of which is usually a deterministic differential equation or Fokker-Planck equation for the mean concentrations of the constituent particles. These equations—reaction-diffusion equations—are often studied first as a means of characterizing the qualitative behavior of the model under examination; they constitute a mean-field theory for the model.

For RD models without disorder in the reaction rates, there exists a well-developed field-theoretic machinery which can be used to treat fluctuations [13,14] and determine (for instance) the critical behavior at the active to absorbing state transition. However, the effects of quenched disorder in the reaction rates on the critical behavior of RD models have been difficult to determine. A straightforward renormalization group treatment leads to runaway flows [14,20], but some progress has been made using simulations [21–25] and real-space renormalization group methods [26,27]. Disorder effects on RD fronts have also been studied, mostly for the

case in which the disorder is time dependent (“annealed”) and the system admits a front solution in the absence of noise [28–31]. However, a few studies have been made of the effects of quenched disorder on RD fronts [32], and some attention has been devoted to the interesting case of noise-induced fronts [33,34].

Although RD models without disorder display a rich variety of behaviors, there are some signs that their utility as models of real-world systems is somewhat limited. One such sign is the dearth of experimental evidence of the directed percolation (DP) class of active to absorbing state phase transitions; one cause of this may be that any real-world system has disorder, and any amount of disorder changes the nature of the DP transition [14,35]. It seems that in order to accurately model some real-world systems, one must include disorder. This obviously makes the analysis of a given RD model much harder, as the field-theoretic machinery cannot be applied (or at the very least is quite cumbersome to apply). If one is also interested in a parameter regime in which internal noise or stochasticity is important, then the model becomes even more challenging to solve, as mean-field methods fail. With both mean-field theory and perturbative field-theoretic tools inapplicable, one must dig deeper into the proverbial toolbox in these situations.

In this work, we will consider transport in an RD model in which quenched disorder and internal noise each plays a role. In order to tackle this model analytically, we will use tools drawn from a wide variety of sources as well as analogies to a number of other systems, including doped semiconductors in the hopping conduction regime and first passage percolation on a lattice. We will also present simulation results which by and large confirm our analytical predictions. Some of the material contained in this paper has been described by us in less detail in an earlier presentation [36].

B. Our model: Oases and deserts

Our model possesses a mean-field limit defined by the generalized Fisher–Kolmogorov–Petrovskii–Piskunov (KPP) equation

*missel@uiuc.edu

†dahmen@uiuc.edu

$$\frac{\partial c(\mathbf{x}, t)}{\partial t} = D \nabla^2 c(\mathbf{x}, t) - \mathbf{v} \cdot \nabla c(\mathbf{x}, t) + U(\mathbf{x})c(\mathbf{x}, t) - qc(\mathbf{x}, t)^2, \quad (1)$$

where $c(\mathbf{x}, t)$ represents the population density (mean particle concentration), D is the diffusion constant, \mathbf{v} is a spatially uniform convection velocity (representing the flow of some liquid in which the particles exist), $U(\mathbf{x})$ is a spatially inhomogeneous growth term fixed in time, and $q \equiv b\ell_0^d$ is a competition term (b is a competition rate and ℓ_0 is the microscopic length scale at which two particles will compete with one another). One of the simplest cases to consider is when $U(\mathbf{x}) = -z$ everywhere except a small patch near the origin, where $U(\mathbf{x}) = y$. The region of positive growth rate near the origin is called an ‘‘oasis,’’ while the rest of space is termed the ‘‘desert.’’ This model was previously studied by Nelson and co-workers [4,5], and a microscopic model (the contact process with disorder) with this mean-field limit was studied by Joo and Lebowitz [37]. Each set of researchers found a transition in the $\langle U(\mathbf{x}) \rangle - |\mathbf{v}|$ plane between extinct, localized, and delocalized phases in a finite system with periodic boundary conditions: For high average growth rate and high convection velocity, they observed a delocalized phase; for low average growth rate and high convection velocity they found that the population became extinct; and for low average growth rate and low convection velocity they found a localized phase. These predictions were tested in a laboratory setting using bacteria protected from harmful uv light (the ‘‘desert’’) by a mask (the ‘‘oasis’’); the experiments largely confirmed the theoretical predictions summarized above [38].

In this paper, we will examine the nature of transport in a system consisting of many identical oases distributed randomly at low density in a desert. We term this low oasis density regime ‘‘hostile,’’ the opposite case in which oases fill up most of space we call ‘‘fertile.’’ Because transport between oases in such a system involves the movement of a low population density, fluctuations about the mean-field theory (discreteness effects) are important. We will thus be examining a particular stochastic process with a mean-field limit given by (1). This process is easiest to introduce on a $d=1$ lattice; the generalization to higher dimensions is trivial. Identical particles (labeled A) occupy lattice sites without occupation number limits and are allowed to undergo the following processes: Hopping to either side with rate $w/2$ (total hopping rate of w); death ($A \rightarrow 0$) with rate z if in the desert; reproduction ($A \rightarrow 2A$) with rate y if on an oasis; and competition and/or coagulation ($2A \rightarrow A$) with rate b everywhere. This process is governed by a master equation for the joint probability $P(\{c\}, t)$ to have occupation numbers $\{c\} \equiv \{\dots, c_{\nu-1}, c_\nu, c_{\nu+1}, \dots\}$ on the lattice points ν at time t .

Let us now present a brief outline of this paper: In Sec. II, we will examine the nature of growth near a single oasis, and we will also briefly discuss in this section the problem of extinction. In Sec. III, we will look at transport between two oases. By using the fact that the $2A \rightarrow A$ competition process is unimportant far away from an oasis where the population is low, we will be able to devise a simpler model which captures the transport characteristics of the full model for

large oasis separation. In Sec. IV, we will finally tackle the problem of transport in a system with many oases. By employing an analogy with the problem of hopping conduction in doped semiconductors, we will estimate the time taken for a population to cross a large system. Finally, we offer a summary of our results along with some remarks in Sec. V.

II. GROWTH NEAR ONE OASIS

A. Mean-field description

We begin with a study of the nature of population growth near a single oasis in mean-field theory. Consider a system on a $d=1$ lattice with a single oasis of $2a+1$ lattice points centered at the origin (we will assume from here on that there is no convection). One can manipulate the master equation to arrive at an equation for the time evolution of the average particle concentration $\langle c_\nu \rangle(t)$ (ν is a lattice point),

$$\frac{\partial \langle c_\nu \rangle(t)}{\partial t} = \frac{w}{2} [\langle c_{\nu+1} \rangle(t) + \langle c_{\nu-1} \rangle(t) - 2\langle c_\nu \rangle(t)] + (y_\nu - z_\nu) \langle c_\nu \rangle(t) - b \langle c_\nu (c_\nu - 1) \rangle(t). \quad (2)$$

In the above equation, $y_\nu = y$ on the oasis and 0 elsewhere, while $z_\nu = z$ in the desert and 0 everywhere else. In order to obtain a ‘‘mean-field’’ description of our system, we replace the term $\langle c_\nu (c_\nu - 1) \rangle$ with $\langle c_\nu \rangle^2$. This replacement should work well when the population is large—i.e., near the oasis—since we would expect the relative fluctuations in particle number to be smaller in this case. With this replacement, we can write a mean-field equation for $\bar{c}(\nu, t) \equiv \langle c_\nu \rangle(t)$,

$$\frac{\partial \bar{c}(\nu, t)}{\partial t} = \frac{w}{2} [\bar{c}(\nu+1, t) + \bar{c}(\nu-1, t) - 2\bar{c}(\nu, t)] + [y(\nu) - z(\nu)]\bar{c}(\nu, t) - b\bar{c}(\nu, t)^2. \quad (3)$$

It is easier to consider the continuum version of this equation, which is obtained by introducing a lattice spacing ℓ_0 and redefining $b \rightarrow q/\ell_0$, $\nu \rightarrow x/\ell_0$, and $\bar{c}(\nu, t) \rightarrow \bar{c}(x, t)\ell_0$. The diffusion constant D is defined as $w\ell_0^2/2$. This leads to a $d=1$ version of (1),

$$\frac{\partial \bar{c}(x, t)}{\partial t} = D \frac{\partial^2 \bar{c}(x, t)}{\partial x^2} + [y(x) - z(x)]\bar{c}(x, t) - q\bar{c}(x, t)^2. \quad (4)$$

There are two things we would like to know: First, what does the mean-field concentration $\bar{c}(x, t)$ look like as $t \rightarrow \infty$? Second, what is the time scale on which a small population grows into a substantial population? Solving analytically for $\bar{c}(x, t)$ for all times is not feasible, but it is possible to solve for the steady state $t \rightarrow \infty$ solution $\bar{c}(x, t = \infty) \equiv \bar{c}_{ss}(x)$ and thus answer the first question. This function is given by

$$\bar{c}_{ss}(x) = \bar{c}_{ss}(0) - m_+ \operatorname{sn}^2 \left(\sqrt{\frac{q|m_-|}{6D}} |x|, i \sqrt{\frac{m_+}{|m_-|}} \right), \quad |x| < a,$$

$$\bar{c}_{ss}(x) = \frac{3z}{2q} \operatorname{csch}^2\left(\frac{\kappa}{2}(|x| - a) + C\right), \quad |x| > a, \quad (5)$$

where $\operatorname{sn}(u, k)$ is a Jacobi elliptic function, $\kappa \equiv \sqrt{z/D}$, $\bar{c}_{ss}(0)$ is the steady-state population at the origin, $C = \operatorname{csch}^{-1}[\sqrt{2q\bar{c}_{ss}(a)}/3z]$ [$\bar{c}_{ss}(a)$ is the steady-state population at the edge of the oasis], and m_{+-} are defined as $\frac{1}{2}\{3\bar{c}_{ss}(0) - 3y/2q \pm \sqrt{[3y/2q - \bar{c}_{ss}(0)][3y/2q + 3\bar{c}_{ss}(0)]}\}$. The constants $\bar{c}_{ss}(0)$ and $\bar{c}_{ss}(a)$ can be found by matching the solutions and their derivatives at $|x|=a$. Numerically, we have found that an excellent approximation to $\bar{c}_{ss}(0)$ is $\bar{c}_{ss}(0) \approx (y - y_c)/q$, where y_c is the minimum growth rate at which the population does not die off as $t \rightarrow \infty$ when $q=0$. This cutoff can be found by solving (4) with $q=0$ (see Appendix A), which leads to the following transcendental equation for y_c :

$$y_c = z \cot^2\left(\sqrt{\frac{y_c}{D}} a\right). \quad (6)$$

At large distances from the oasis ($|x| \gg a$), $\bar{c}_{ss}(x) \approx \bar{c}_\infty e^{-\kappa|x|}$, where $\bar{c}_\infty = 4\gamma^2 \bar{c}_{ss}(a) e^{\kappa a}$ [$\gamma^{-1} = 1 + \operatorname{csch}(C)$]. In the limit of high growth rate— $y \rightarrow \infty$ with all other rates fixed— $\bar{c}_{ss}(a) \rightarrow \infty$ and $\bar{c}_\infty \rightarrow 6ze^{\kappa a}/q$.

In higher dimensions, we consider a hyperspherical oasis of radius a . It is not possible to solve exactly the $t \rightarrow \infty$ nonlinear mean-field equation for $d > 1$, but it is easy to ascertain the asymptotic behavior of $\bar{c}_{ss}(\mathbf{x})$ far away from the oasis. To do so, we drop the nonlinear term from the mean-field equation (1) under the assumption that $\bar{c}_{ss}(\mathbf{x})$ is small far from the oasis. This leads to the linear equation

$$0 = D\nabla^2 \bar{c}_{ss}(\mathbf{x}) - z\bar{c}_{ss}(\mathbf{x}), \quad (7)$$

which is valid far away from the oasis. In two dimensions, this is solved by $\bar{c}_{ss}(\mathbf{x}) \approx \bar{c}_\infty K_0(\kappa r)$, where $r = |\mathbf{x}|$ and K_0 is a modified Bessel function of the first kind. In three dimensions, $\bar{c}_{ss}(\mathbf{x}) \approx \bar{c}_\infty e^{-\kappa r}/\kappa r$. Because finding an exact solution for the entire space (including $r < a$) is no longer possible for $d=2$ or 3, we cannot write an analytic expression for the prefactors \bar{c}_∞ in front of these asymptotic functional forms.

The question of the time scale on which a small population grows into a substantial population has been addressed by Nelson and co-workers [4,5]. They analyzed the eigenvalue spectrum of the linearized ($q=0$) version of (1) and found that the largest eigenvalue Γ_0 is given by [5]

$$\Gamma_0 = (y + z)f[\sqrt{D/a^2(y + z)}] - z, \quad (8)$$

where $f(x)$ is a monotonically decreasing function of x which goes as $1 - \pi^2 x^2/4$ for $x \ll 1$ and $1/x^2$ for $x \gg 1$. In the limit of large y , then, $\Gamma_0 \approx y$, and the time scale on which a small population grows up is $\sim 1/y$.

B. Fluctuations and extinction

It has been known for some time that fluctuations can drive a system to extinction even when mean-field theory predicts a stable active state. In the case of a continuous homogeneous system with the same reactions as our system— $A \rightarrow 2A$ with rate y , $A \rightarrow 0$ with rate z , and $2A \rightarrow A$ with rate b —there is an active phase only when $z - y < r_c$,

where r_c depends on dimension but is less than zero for $d = 1, 2, 3$ [14]. Mean-field theory, on the other hand, predicts an active phase for $y > z$; fluctuations drive the critical growth rate up. The disparity between mean-field and stochastic behavior is even greater in the case of a $d=0$ system: Mean-field theory predicts a $t \rightarrow \infty$ steady state which is reached for any nonzero initial condition when $y > z$, but solving the master equation leads to the conclusion that, for any $z > 0$, the population will eventually become extinct [19]. The mean extinction time in this case can be calculated exactly as a function of y , z , b , and the starting population n_0 , although the resulting expression is cumbersome to work with [19].

For the case of a single oasis in an infinite desert, it seems clear that the population will become extinct as $t \rightarrow \infty$ for $d = 1, 2, 3$: The finite oasis cannot compete with the infinite desert, regardless of how high the growth rate y is. For the problem we will be considering, it is important that the oases not die out too early, and thus we need to know the dependence of the mean extinction time on the various parameters of the problem. The field-theoretic tools used to analyze systems with translational invariance are hard to apply to this case, as are the various methods (see Ref. [39] for one such method) used to analyze $d=0$ systems. Nonetheless, we can try to place a lower limit on the extinction time. To do so, we will return to the lattice case in one dimension; our results will be applicable to the continuum case and to other dimensions.

Consider the case of a perfectly deadly desert, $z \rightarrow \infty$. This effectively turns our system into a finite system with $2a+1$ lattice points and absorbing boundaries. The “effective” death rate is of the order of w , the hopping rate. Now consider a $d=0$ system with the same birth and competition rates which has a death rate of w , the hopping rate in our original system. Our $d=1$ system will certainly live longer than this system, on average: The number of events needed to extinguish the population completely is much larger. As mentioned above, the mean extinction time for this $d=0$ system can be calculated explicitly, with the result that $T_{\text{extinct}} \sim e^{cy}$, where c is a constant, for large y [19]. This suggests that the mean extinction time should rise at least exponentially with y in our one oasis problem when y is large. By choosing a large y , then, we can ensure that extinction will not invalidate our results. From here on, we will assume that the growth rate on the oases is large enough that extinction is unlikely on the transport time scales in question.

III. TRANSPORT BETWEEN TWO OASES

A. Transport as a first passage process

Our eventual goal is to understand the transport of a population across a system filled with oases at low density. The first step towards such an understanding is to determine the nature of transport between two oases. Consider two oases of radius a in d dimensions. The center of one oasis is located at the origin, and the center of the other oasis is located at position \mathbf{R} . At $t=0$, the first oasis is populated and the second oasis is empty. We wish to find the infection time—that is, the time it takes for a population to take hold and reach a

significant level on the second oasis. This time can be roughly broken into two parts: T_{transit} , the time it takes particles from the first oasis to reach the second oasis; and T_{growth} , the time it takes the population to rise to a significant level once the second oasis has been reached. We will assume that the first particle to reach the second oasis will reproduce and that its offspring will not die out; in other words, we will take T_{transit} to be the first passage time (FPT) of the process. This assumption can be satisfied in two ways: The first way is simply to make the growth rate y of the oases very high. In this case, it is possible to estimate how the survival probability increases as y increases. Consider again the case of a very deadly desert in a $d=1$ lattice system with hopping rate w : If the particle diffuses off the oasis, it is certainly dead; thus, there is an effective death rate of order w . For the case of a very small oasis, then, a toy model of the oasis is a $d=0$ system with death rate of w . For this case, it is known that the survival probability goes like $1-w/y$ [19], and thus making y very high assures that the population will take hold and survive. A second way of satisfying our assumption is to seed the oases with a second species of particles, B , which interact with the A particles via the reaction $A+B \rightarrow 2A$ at a very high rate.

The time T_{growth} that it takes the initially small population on the second oasis to grow to a macroscopic size should go roughly like $1/y$ for large y , and so choosing a large y should also serve to make $T_{\text{growth}} \ll T_{\text{transit}}$. For the remainder of the paper, we will assume that y is large enough so that this is the case. Note that by taking y to be very high, we have done three things: First, we have ensured that a small population which reaches a new oasis grows into a sizable population and does not die out, which allows us to identify the first passage time with the transit time; second, we have made the time for this growth small compared to the transit time; and finally, as mentioned in the preceding section, we have ensured that extinction will only occur on a time scale much larger than the one associated with transit.

Consider the case where the two oases are close together: Particles from the first oasis diffuse out in a front, its amplitude decaying due to the death term in the desert and competition effects. However, so long as the second oasis is close enough that the edge of the front is almost certain to possess many particles (the number will vary from realization to realization of the stochastic process), the transit time should simply go as R , the oasis separation. However, once R is well above some length scale we will call R_{lin} , this is no longer true: The front simply does not exist in most realizations of the system, as the number of particles present at this distance from the first oasis is quite small for all times. In this regime, the second oasis is reached not by a front but by a stray particle (or some stray particles) that manages to make it through the desert; it is essentially a noise-induced growth process. R_{lin} can thus be roughly defined as the distance from the oasis at which the large-time average concentration falls to $1/\ell_0^d$. We have already analyzed the mean-field equations for the average concentration as $t \rightarrow \infty$, and found that, except in $d=1$, there are no closed-form solutions. In one dimension, setting the mean-field $t \rightarrow \infty$ average concentration (5) for large y equal to $1/\ell_0$ and solving for R_{lin} leads to

$$R_{\text{lin}} = a + \sqrt{\frac{4D}{z}} \operatorname{csch}^{-1} \left(\sqrt{\frac{2b}{3z}} \right), \quad (9)$$

where a is the radius of the oases. In the limit of large z/b , this simplifies to $R_{\text{lin}} \approx a + \sqrt{D/z} \ln(6z/b)$, where b is q/ℓ_0 . If y is smaller, the relevant length scale will also be smaller. We believe that this length scale should be of the same order of magnitude in higher dimensions, and so (9) should also provide a rough estimate of R_{lin} for $d=2$ and 3.

B. Simpler linear model with a source

As we move further from the first oasis, the competition process $2A \rightarrow A$ becomes less and less important, especially if b is small compared to the other rates in the problem. Due to this fact, it is natural to wonder if ignoring these interactions altogether might be the first step in the creation of a tractable model with the same large distance first passage properties as the full model with competition. We will now propose such a model, which has been discussed by us in an earlier work [36]: Consider replacing the first oasis with desert, and then placing a point source in the middle that produces noninteracting particles at some average rate g . For an appropriately chosen g , the mean flux of particles past the surface at R_{lin} should match that of the model with competitions; beyond that point, the model with a source differs from the model with competitions only in that it ignores the rare annihilation interactions between particles. We will show that, for an appropriately chosen g , this model—which we will refer to as the linear model with a source—accurately captures the first passage properties of the full nonlinear model with competition.

As with the full nonlinear model with competition (hereafter referred to as the nonlinear model), it is useful to analyze the mean-field behavior of the linear model with a source. The time evolution of the average number of particles $\bar{n}(\nu, t)$ is described by

$$\begin{aligned} \frac{\partial \bar{n}(\nu, t)}{\partial t} = & \frac{w}{2} [\bar{n}(\nu+1, t) + \bar{n}(\nu-1, t) - 2\bar{n}(\nu, t)] - z\bar{n}(\nu, t) \\ & + g \delta_{\nu,0}. \end{aligned} \quad (10)$$

We will study the continuum version of this equation in detail in one, two, and three dimensions. Taking the continuum limit of (10) (and changing $\partial_x^2 \rightarrow \nabla^2$ for $d > 1$) results in

$$\frac{\partial \bar{n}(\mathbf{x}, t)}{\partial t} = D \nabla^2 \bar{n}(\mathbf{x}, t) - z \bar{n}(\mathbf{x}, t) + g \delta^d(\mathbf{x}). \quad (11)$$

Unlike the mean-field equation for the model with competitions, this equation can be solved exactly in all dimensions. If we assume an initial condition with no particles present, a Laplace transform in time and Fourier transform in space leads to

$$\bar{n}(\mathbf{k}, s) = \frac{g}{s(s + D\mathbf{k}^2 + z)}. \quad (12)$$

We are interested in the long-time, steady-state behavior in all dimensions. Multiplying by s , letting $s \rightarrow 0$, and trans-

forming back to real space gives the following solutions for $\bar{n}_{ss}(\mathbf{x}) \equiv \bar{n}(\mathbf{x}, t \rightarrow \infty)$:

$$\bar{n}_{ss}(x) = \frac{g e^{-\kappa|x|}}{\sqrt{4Dz}} \quad (1D),$$

$$\bar{n}_{ss}(r) = \frac{gK_0(\kappa r)}{4\pi D} \quad (2D),$$

$$\bar{n}_{ss}(r) = \frac{g e^{-\kappa r}}{4\pi D r} \quad (3D). \quad (13)$$

There is one additional case of interest: The $d=1$ lattice case. The relevant mean-field equation in this case is simply (10). After a Laplace transform, we are left with a difference equation which can be solved with the ansatz $\bar{n}(\nu+1, s) = e^{-f(s)} \bar{n}(\nu, s)$ for $\nu > 0$. The solution is

$$\bar{n}(\nu, s) = \frac{g e^{-f(s)|\nu|}}{s w \sinh[f(s)]}, \quad (14)$$

where $f(s) = \cosh^{-1}[1 + (s+z)/w]$. The $t \rightarrow \infty$ behavior of $\bar{n}(\nu, t)$ is thus

$$\bar{n}_{ss}(\nu) \equiv \bar{n}(\nu, t \rightarrow \infty) = \frac{g e^{-f|\nu|}}{w \sinh(f)}, \quad (15)$$

where $f \equiv f(0)$.

The functional forms of the continuum solutions in (13) are the same as those of the solutions for the asymptotic ($r \gg a$) steady-state nonlinear ($b \neq 0$) equations discussed in Sec. II A. For a properly chosen creation rate g , the mean-field solutions of the two models should match at long distances. We will use this method of matching mean-field solutions to determine g for the purposes of making numerical predictions of first passage properties in the nonlinear model.

C. Analytic predictions from the linear model with a source

With a method in place for determining g from the parameters of the nonlinear model, it is now possible to use the linear model with a source to make quantitative predictions about first passage properties of the two oasis system. We begin by noting that, since the particles in the linear model with a source are noninteracting, the full multiparticle first passage time probability density function (FPT PDF) $f_N(\mathbf{x}, t)$ —that is, the probability per unit time that the first particle from the first oasis reaches the second oasis between t and $t+dt$ —can be written in terms of the one-particle FPT PDF $f_1(\mathbf{x}, t)$. [Note that the vector \mathbf{x} is a stand-in for all the geometric particulars of the system. For instance, for a spherical or circular oasis, $f_N(\mathbf{x}, t)$ depends on the distance of the center of the oasis from the origin R and the radius a of the oasis. These geometrical particulars are not important for our present discussion, and so we express f_N as a function of the generic vector \mathbf{x} .] This is accomplished as follows: Assume the source is at the origin, and that it releases N particles at regular intervals Δt . Define $S(\mathbf{x}, t) = 1 - \int_0^t dt' f_1(\mathbf{x}, t')$ to be the probability that a particular particle released from the origin at $t=0$ has not reached the target oasis by time t . If we define $P_{\text{none}}(\mathbf{x}, t)$ to be the probability that no particles from the source have hit the target oasis by time t , then

$$P_{\text{none}}(\mathbf{x}, t) = \prod_{\tau=0, \Delta t, \dots}^t [S(\mathbf{x}, \tau)]^N. \quad (16)$$

Taking the logarithm of this expression gives

$$\ln[P_{\text{none}}(\mathbf{x}, t)] = \sum_{\tau=0, \Delta t, \dots}^t g \Delta t \ln[S(\mathbf{x}, \tau)], \quad (17)$$

where $g \equiv N/\Delta t$ is the creation rate [40]. Taking the limit $\Delta t \rightarrow 0$ with g fixed and exponentiating both sides leads to a closed equation for $P_{\text{none}}(\mathbf{x}, t)$ in terms of $S(\mathbf{x}, t)$,

$$P_{\text{none}}(\mathbf{x}, t) = \exp\left(g \int_0^t dt' \ln S(\mathbf{x}, t')\right). \quad (18)$$

Since we are interested in oasis separations large enough that a given single particle has a low probability of ever reaching the second oasis, $S(\mathbf{x}, t)$ is close to 1 even as $t \rightarrow \infty$. This allows us to approximate $\ln S(\mathbf{x}, t) = \ln[1 - P_{\text{hit}}(\mathbf{x}, t)]$ by $-P_{\text{hit}}(\mathbf{x}, t)$, leading to a simpler expression for $P_{\text{none}}(\mathbf{x}, t)$,

$$P_{\text{none}}(\mathbf{x}, t) \simeq \exp\left(-g \int_0^t dt' (t-t') f_1(\mathbf{x}, t')\right). \quad (19)$$

The full FPT PDF $f_N(\mathbf{x}, t)$ is simply $-\partial_t P_{\text{none}}(\mathbf{x}, t)$.

There is one more useful way to write P_{none} : Since the integral appearing in the exponent in (19) is a convolution of t and $f_1(\mathbf{x}, t)$, its Laplace transform is simply a product of the two functions' individual Laplace transforms. Explicitly,

$$P_{\text{none}}(\mathbf{x}, t) \simeq \exp\{-g \mathcal{L}^{-1}[f_1(\mathbf{x}, s)/s^2]\}, \quad (20)$$

where $\mathcal{L}^{-1}[u(s)]$ is the inverse Laplace transform of $u(s)$ and $f_1(\mathbf{x}, s)$ is the Laplace transform in time of $f_1(\mathbf{x}, t)$. Often it is easier to compute $f_1(\mathbf{x}, s)$ than $f_1(\mathbf{x}, t)$, and in these cases (20) can be very useful.

In order to make predictions using (19) or (20), it is necessary to compute the one-particle FPT PDF $f_1(\mathbf{x}, t)$. We will do this now for the continuum case in all relevant dimensions and the lattice case in $d=1$. We will start with the continuum case. The diffusion equation governing the probability distribution $p_1(\mathbf{x}, t)$ of a particle released into the desert from the origin at $t=0$ is

$$\frac{\partial p_1(\mathbf{x}, t)}{\partial t} = D \nabla^2 p_1(\mathbf{x}, t) - z p_1(\mathbf{x}, t), \quad (21)$$

with boundary condition $p_1(\text{oasis surface}, t) = 0$. This boundary condition is of course not true in the model—particles arriving at the oasis will not immediately die—but it is used as a device to extract first passage properties. By writing $p_1(\mathbf{x}, t) = \phi_1(\mathbf{x}, t) e^{-zt}$, it is possible to eliminate the death term in (21) and arrive at a simple diffusion equation for $\phi_1(\mathbf{x}, t)$. The FPT PDF $f_1(\mathbf{x}, t)$ can be obtained by considering the flux of probability into the oasis [41],

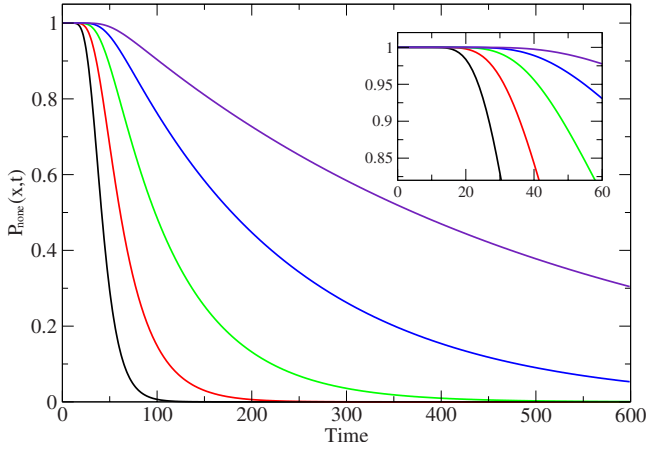


FIG. 1. (Color online) Main window: Plot showing $P_{\text{none}}(x, t)$ in $d=1$. The lines represent, from left to right, the function for $x=16, 18, 20, 22,$ and 24 . Inset: A blowup showing the early-time behavior of P_{none} .

$$f_1(\mathbf{x}, t) = D \int_{\text{surface}} dA \hat{n} \cdot \nabla \phi_1(\mathbf{x}, t) e^{-z t}, \quad (22)$$

where dA is an element of the oasis surface and \hat{n} is a unit vector pointing out from the oasis. Since $\phi_1(\mathbf{x}, t)$ is the solution to a simple diffusion equation, $D \int dA \hat{n} \cdot \nabla \phi_1(\mathbf{x}, t) = f_1^{\kappa=0}(\mathbf{x}, t)$, the FPT PDF in the case where there is no desert. This fact can be combined with (22) to arrive at the conclusion

$$f_1(\mathbf{x}, t) = f_1^{\kappa=0}(\mathbf{x}, t) e^{-z t}. \quad (23)$$

The Laplace-transformed FPT PDF $f_1(\mathbf{x}, s)$ is thus related to the $z=0$ function by

$$f_1(\mathbf{x}, s) = f_1^{\kappa=0}(\mathbf{x}, s + z). \quad (24)$$

These results are convenient due to the fact that, for circular or spherical oases, exact solutions exist for $f_1^{\kappa=0}(\mathbf{x}, t)$.

In one dimension, $f_1^{\kappa=0}(x, t) = |x| e^{-x^2/4Dt} / \sqrt{4\pi Dt^3}$ [41]. Using this result along with (23), plugging into (19), and performing the integration [42] gives

$$P_{\text{none}}(x, t) \approx \exp\left(-\frac{g}{4z} (e^{\kappa|x|} \zeta^+ \operatorname{erfc}(\zeta^+/\sqrt{4zt}) - e^{-\kappa|x|} \zeta^- \operatorname{erfc}(\zeta^-/\sqrt{4zt}))\right), \quad (25)$$

where $\zeta^\pm = \zeta^\pm(x, t) = \kappa|x| \pm 2zt$. This function is shown in Fig. 1. For large times, $P_{\text{none}}(x, t) \approx \exp(-g e^{-\kappa|x|} t)$. The j th moment of $f_N(x, t)$ is given by $\langle T^j(x) \rangle = j \int_0^\infty dt P_{\text{none}}(x, t) t^{j-1}$; although it is not possible to perform this integral analytically, we can extract its $|x| \rightarrow \infty$ (large oasis separation) behavior (see Appendix B),

$$\langle T^j(x) \rangle = j! \frac{e^{\kappa|x|j}}{g^j} \quad (1D \text{ continuum}). \quad (26)$$

In two and three dimensions, it becomes more convenient to solve for $f_1(\mathbf{x}, s)$. The single-particle FPT PDF is a func-

tion of the separation of the center of the target oasis from the origin \mathbf{R} and the radius of the oasis a , so we will from now on write it as $f_1(R, a, t)$, where $R=|\mathbf{R}|$. The FPT PDF in frequency space in the absence of a desert ($z=0$) is known for these cases [41]; using (24) gives

$$f_1(R, a, s) = \left(\frac{a}{R}\right)^{d/2-1} \frac{K_{d/2-1}\left(\sqrt{\frac{s+z}{D}} R\right)}{K_{d/2-1}\left(\sqrt{\frac{s+z}{D}} a\right)}, \quad (27)$$

where K_n is the n th-order modified Bessel function of the first kind. This equation also holds in $d=1$; redefining $x=R-a$ and using the definition of $K_{1/2}$ leads to the correct Laplace transform of the $d=1$ FPT PDF.

In $d=2$, using (20) and (27) gives

$$P_{\text{none}}(R, a, t) \approx \exp\left(-\frac{g}{2\pi i} \int_{\mathcal{L}} ds \frac{e^{st} K_0\left(\sqrt{\frac{s+z}{D}} R\right)}{s^2 K_0\left(\sqrt{\frac{s+z}{D}} a\right)}\right). \quad (28)$$

Appendix B contains the details of the evaluation of (28) and the extraction of the $R \rightarrow \infty$ moments of $f_N(R, a, t)$; we will simply quote the results here. The large t behavior of P_{none} is given by $P_{\text{none}}(R, a, t) \approx \exp\{-g[K_0(\kappa R)/K_0(\kappa a)]t\}$. The moments of $f_N(R, a, t)$ asymptotically approach

$$\langle T^j(R, a) \rangle = j! \left(\frac{K_0(\kappa a)}{g K_0(\kappa R)}\right)^j \quad (2D \text{ continuum}) \quad (29)$$

as $R \rightarrow \infty$.

The three-dimensional case is easy to treat. Since $K_{-n}(z) = K_n(z)$, looking at (27) immediately shows that $f_1(R, a, s)$ for $d=3$ is identical to the $d=1$ case save for a factor of a/R . Making the replacements $|x| \rightarrow R-a$ and $g \rightarrow ga/R$ in (25) gives $P_{\text{none}}(R, a, t)$; making the same replacements gives the $t \rightarrow \infty$ decay $P_{\text{none}}(R, a, t) \approx \exp[-g(a/R)e^{-\kappa(R-a)}t]$. The moments approach

$$\langle T^j(R, a) \rangle = j! \left(\frac{R}{a}\right)^j \frac{e^{\kappa(R-a)j}}{g^j} \quad (3D \text{ continuum}) \quad (30)$$

as $R \rightarrow \infty$.

The final case we will consider is the $d=1$ lattice case. Recall that for this case, w is total hopping rate and the integer ν denotes the lattice point. The single-particle FPT PDF $f_1(\nu, t)$ is [41]

$$f_1(\nu, t) = \frac{|\nu| e^{-(w+z)t} I_\nu(wt)}{t}, \quad (31)$$

where I_ν is the ν th order modified Bessel function of the first kind. It is more convenient to use the frequency space function,

TABLE I. Parameters used in two sets of simulations designed to test the effectiveness of the linear model with a source.

Parameter	Description	Set 1	Set 2
a	Oasis radius	2	2
$R_<$	Minimum distance measured	10	15
$R_>$	Maximum distance measured	30	45
w	Hopping rate	1.0	1.0
y	Birth rate	0.25	7.5
z	Death rate	0.1	0.025
b	Competition rate	0.001	0.1
$c_0(0)$	Starting population	125	37
N_{sims}	Number of runs	5000	1533

$$f_{\downarrow}(\nu, s) = \frac{w^{|\nu|}}{[s + w + z + \sqrt{(s+z)(s+z+2w)}]^{|\nu|}}. \quad (32)$$

Using this together with (20) gives an expression for $P_{\text{none}}(\nu, t)$; the important results are that the function decays as $P_{\text{none}}(\nu, t) \approx \exp(-ge^{-f|\nu|}t)$ as $t \rightarrow \infty$, and that, as in the continuum case, P_{none} cannot be integrated analytically, but an asymptotic analysis shows that, as $|\nu| \rightarrow \infty$,

$$\langle T^j(\nu) \rangle = j! \frac{e^{f|\nu|j}}{g^j} \quad (\text{1D lattice}). \quad (33)$$

In the above expressions, $f = \cosh^{-1}(1 + z/w)$.

D. Simulation results

In order to test the predictions of the linear theory with a source, we wrote a kinetic Monte Carlo (KMC) simulation of the nonlinear model. While it is certainly possible to simulate the continuum model in any dimension either by doing a discrete-space simulation and choosing very small lattice spacings or by using an event-driven algorithm [43], we found it more expedient to do a lattice simulation in $d=1$ and compare with the predictions from the lattice version of the linear model with a source.

The first set of parameters for which we ran simulations is listed in the third column of Table I, and the second set is listed in the fourth column. Each simulation run began with $c_0(0)$ particles placed at the center lattice point (the middle of the oasis) and ended when the lattice point $R_>$ was hit for the first time. At each step of the simulation, an event i with rate

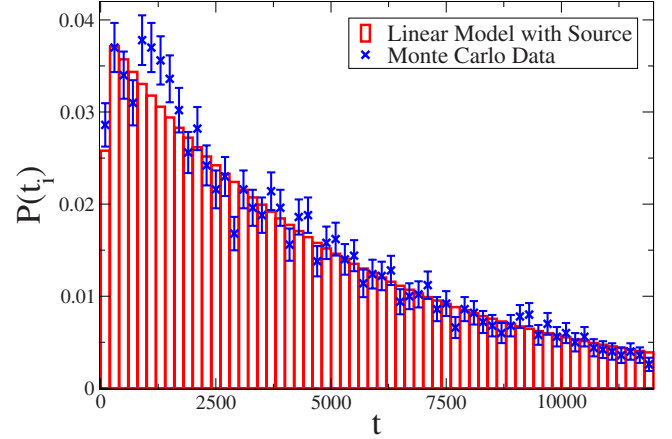


FIG. 2. (Color online) Binned FPT probabilities for $\nu=30$ from both the linear model with a source (red boxes) and Monte Carlo simulations of the nonlinear model (blue lines). The width of each bin is $200/w$, where w is the total hopping rate. The error bars on the simulation data represent sampling error.

r_i was chosen with probability $p_i = r_i / r_{\text{tot}}$ ($r_{\text{tot}} = \sum_i r_i$), the occupation numbers on the lattice sites were updated, and time was advanced by $\Delta t = -\ln(U)/r_{\text{tot}}$, where U is a uniformly distributed random number. To compare the simulation data to the predictions from the linear model with a source, we numerically solved the mean-field equation (3) and matched the large time, large ν tails to the large time tails of the mean-field solution of the linear model with a source given by (15). This resulted in a value of g which could then be used to compute the theoretical FPT predictions.

For small values of the competition parameter b , we found excellent agreement between the predictions from the linear model with a source and the Monte Carlo simulation results. The linear model with a source correctly predicts the lower moments of $f_N(\nu, t)$ for large ν , as shown in Table II. A more stringent test of the power of the linear model with a source is a comparison of its prediction for the full FPT PDF with simulation results. To do this comparison, we integrated $f_N(\nu, t)$ from $(i-1)\Delta t$ to $i\Delta t$ for $i=1, 2, 3, \dots, M$ to obtain a set of probabilities $P(t_i)$ for hitting the point ν for the first time in time bin i . We then compared this prediction with simulation results. The comparison is shown in Fig. 2 for $\nu=30$ for the first set of parameters listed in Table I; it seems clear that the linear model with a source correctly predicts the form of $f_N(\nu, t)$ for this parameter set.

For larger values of b , however, we found that the value of g obtained from matching mean-field solutions leads to an

TABLE II. Comparison of predictions from the linear model with a source for the second and fifth moments of $f_N(\nu, t)$ with Monte Carlo data from the nonlinear model for the first parameter set shown in Table I. The quoted errors represent a 95% confidence interval.

Distance	$\langle T^2 \rangle_{\text{th}}$	$\langle T^2 \rangle_{\text{sim}}$	$\langle T^5 \rangle_{\text{th}}$	$\langle T^5 \rangle_{\text{sim}}$
$\nu=10$	173.739	164.97 ± 2.38404	5.78947×10^5	$(5.38868 \pm 0.208015) \times 10^5$
$\nu=15$	1203.87	1223.91 ± 21.8565	9.67825×10^7	$(9.95067 \pm 0.713879) \times 10^7$
$\nu=20$	14509.5	14691.1 ± 572.021	2.06877×10^{11}	$(1.79262 \pm 0.320831) \times 10^{11}$
$\nu=25$	6.91791×10^5	$(7.00186 \pm 0.424694) \times 10^5$	7.29976×10^{15}	$(8.42756 \pm 3.50113) \times 10^{15}$
$\nu=30$	5.36637×10^7	$(5.13892 \pm 0.321111) \times 10^7$	4.39059×10^{20}	$(4.00704 \pm 1.21406) \times 10^{20}$

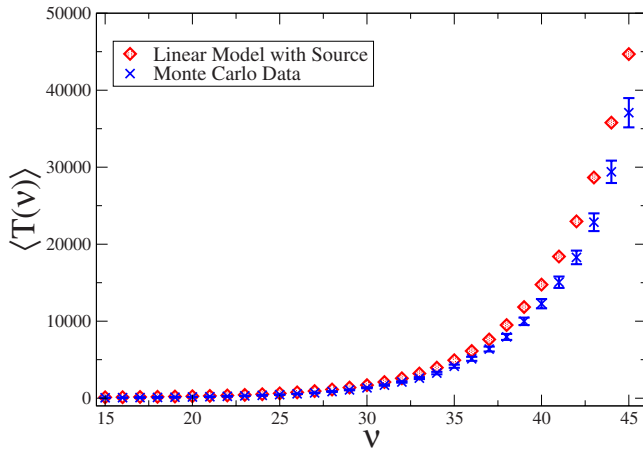


FIG. 3. (Color online) Graph showing the mean FPT as a function of ν for the linear model with a source (red diamonds) and the KMC simulation of the full model with competition (blue marks) for the second parameter set. The error bars represent a 95% confidence level for the simulation mean FPTs.

overestimate of the mean first passage time and all other moments of $f_N(\nu, t)$, as can be seen in Fig. 3, which shows the results of the simulations performed with the second set of parameters from Table I. However, the simulation results still show a mean FPT that rises exponentially like $e^{f\nu}$ for large ν ; it is simply the prefactor g that is off. It is possible, of course, to simply fit the simulation data to the theoretical predictions from the linear model with a source using g as a fit parameter rather than try to get g by matching mean-field solutions. The result of this fitting for the second parameter set is shown in Fig. 4.

In summary: The value of g obtained by matching the tails of the mean-field theory solutions for the two models works well to predict the moments of $f_N(\nu, t)$ only when the competition rate b is relatively small; when it is large, the value of g obtained in this manner is too small, and the linear theory with a source overestimates the mean FPT (and higher

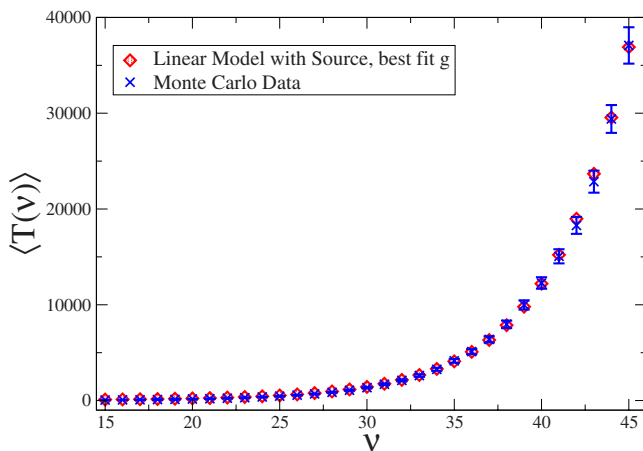


FIG. 4. (Color online) Graph showing the mean FPT as a function of ν for the linear model with a source (red diamonds) and the KMC simulation of the full model with competition (blue marks) for the second parameter set with g chosen to provide the best fit between the data sets.

moments). A little thought shows why this is the case: The competition process in the mean-field theory appears as $-b\bar{c}(\nu, t)^2$, and is thus present at any lattice point at which there is nonzero particle density. However, in reality there need to be two particles present at a site for the competition process to occur; therefore, the mean-field theory overestimates the importance of the competition term at small particle concentrations. The tail of the steady-state mean-field solution is thus “too small,” and matching it with the mean-field solution of the linear model with a source leads to an underestimate of g and an overestimate of the mean FPT. Even for larger values of b , however, the linear theory with a source correctly predicts the shape of $f_N(\nu, t)$ for large values of ν , and it is possible to use g as a fit parameter to make the two models match. Thus, one can conclude that the linear model with a source does indeed capture the important properties of the FPT PDF of the nonlinear model for large oasis separations.

IV. FROM TWO OASES TO MANY

A. Connection with hopping conduction

With results for the two oasis system in hand, we will now turn our attention to a system with many oases at low density. For concreteness, consider a continuum system in d dimensions ($d > 1$) comprised of identical oases of radius a and growth rate γ placed around randomly distributed points with number density n in a desert of death rate z (note that Grassberger has studied the related case of random traps [44], while Redner has studied mixed traps and oases on a lattice [45]). We are interested in the low density regime; that is, the regime in which the average distance between oases $R_{\text{avg}} \propto n^{-1/d}$ is larger than the length scale R_{lin} identified in (9). The oases are allowed to overlap, although this should not happen too often at the low oasis densities being considered. Imagine starting with one or more oases populated at $t=0$ and waiting for a particular oasis or one of a number of oases situated far away to become populated. We will call the total time for this to take place $T_{\text{infection}}$, the infection time. Because of the exponential dependence of the mean FPT on oasis separation for large oasis separations [see (29) and (30)], the time taken to cross the largest oasis separations (or links) on the path should, on average, be much greater than the time taken to cross the shorter links. The situation is somewhat analogous to that of hopping conduction in doped semiconductors [46]: The oases in this system play the role of the impurity sites in the semiconductor, and the mean transit time between oases is akin to the resistance between impurity sites. In doped semiconductors, the resistance between impurity sites depends exponentially on their separation like $e^{\alpha R}$, where R is the impurity separation and $\alpha \equiv 2/a$, where a is an effective Bohr radius describing the width of the impurity wave functions [46]. This is similar to the way the mean transit time (and, indeed, all other moments of the distribution for large separation) depends exponentially on oasis separation in the oasis system. There are a couple of significant differences between the two systems: First, there is no equivalent in the semiconductor problem of the growth time, the time needed for the population on a

newly inhabited oasis to rise to a significant level; second, the resistances between impurity sites are not the averages of stochastic variables such as the mean transit times, but rather definite quantities. The first of these differences is insignificant in the limit we are considering since it has already been assumed that T_{growth} is much smaller than a typical value of T_{transit} for oases separated by a large distance. The second difference is more important, and some of its implications will be discussed in detail later in this paper.

The problem of determining the resistivity (or conductivity) of a doped semiconductor in the hopping regime was first tackled satisfactorily using ideas from percolation theory by Ambegaokar and co-workers [47,48]. They found that the resistivity is dominated by the largest links in the network of impurity sites spanning the system. Any links with much larger resistances are effectively shunted by the smaller resistances, and are not important in determining the macroscopic resistivity. The size of the largest link R_{max} in the spanning cluster can be determined using continuum percolation theory; this length varies from sample to sample, but has a well-defined limit as the system size goes to infinity [46],

$$R_{\text{max}} = \left(\frac{B_c(d)}{nV_d} \right)^{1/d}, \quad (34)$$

where $B_c(d)$ is the dimensionally dependent bonding criterion, V_d is the volume of a d -dimensional unit hypersphere, and n is the number density of impurity sites. The quantity $B_c(d)$ has an interpretation as the mean number of connected neighbors for members of the percolation cluster, and is equal to ≈ 4.5 in $d=2$ and ≈ 2.7 in $d=3$ [46].

The network which carries the bulk of the current in the system—the current-carrying cluster—has as its largest links those links with resistance not much greater than $e^{\alpha R_{\text{max}}}$ —that is, links of size $\approx R_{\text{max}} + 1/\alpha$. The correlation length of this cluster is denoted by L_0 , and is given (up to numerical prefactors of order 1) by [46]

$$L_0 \approx \frac{(\alpha R_{\text{max}})^\nu}{n^{1/d}}, \quad (35)$$

where $\nu=4/3$ in $d=2$ and ≈ 0.88 in $d=3$.

To determine the resistivity of the system, it is necessary to know something about the structure of the cluster—specifically, it is necessary to know what the typical separation of large links is. One model of the cluster structure is the links-nodes-blobs picture [46,49], which suggests that the cluster can be thought of as a network of nodes separated by a distance on the order of L_0 connected by one-dimensional links and clusters (or blobs) of links. Since the resistance of a link depends exponentially on its length, the largest one-dimensional links of approximate size R_{max} largely determine the resistance between nodes. If a large chunk of material of linear size $L \gg L_0$ has its resistance Ω measured, Ω should be $\sim (L/L_0)^{2-d} e^{\alpha R}$, since there are $\sim (L/L_0)^{d-1}$ chains of resistors connecting the edges of the system, each with resistance $\sim (L/L_0) e^{\alpha R}$. The resistivity ρ is then given by [49–51]

$$\rho = L^{d-2} \Omega = e^{\alpha R} L_0^{d-2}. \quad (36)$$

In addition to being the correlation length of the current-carrying cluster, L_0 is also the length scale at which sample-to-sample variations in αR_{max} become relatively small, of order 1 [46]. That is, if $R_{\text{max}}(L)$ is defined as the largest link in the cluster that spans a finite system of size L , then the width of the probability distribution for $R_{\text{max}}(L)$ becomes small around $L=L_0$. Above the length scale L_0 , the system can be regarded as homogeneous, and so the resistivity of a large system of size $L \gg L_0$ is roughly equal to the resistivity of a system of size L_0 ; this fact is captured in (36).

B. Dynamics of transport in a macroscopic system

Now we return to the problem of oases in a desert. Recall that the dominant contribution to the transit time in any dimension comes from the exponential $e^{\kappa R}$ with $\kappa \equiv \sqrt{z/D}$; thus, substituting κ for α in (35) gives a length scale which can be identified with the typical separation between large oasis separations:

$$L_0 \approx \frac{(\kappa R_{\text{max}})^\nu}{n^{1/d}}, \quad (37)$$

where n is now the number density of oases. Consider a system of size L_0 with one oasis initially infected at one edge of the system. In the hopping conduction problem, the goal is to find the resistance between the edges of the system; in the oasis problem, it is to find the first passage time between the starting oasis and either a specific oasis on the opposite edge or any oasis in a thin layer close to the opposite edge. Unlike the hopping conduction problem, the oasis problem is dynamic in nature; an additional difference is that, as mentioned previously, the first passage times are random variables with a distribution whose mean increases exponentially with oasis separation rather than fixed resistances with an exponential dependence on link size. The mean FPT across the system is thus an average of a minimum: For a fixed set of oases, each realization of the dynamic process yields a path with minimal first passage time which may differ from the paths from other realizations. However, there is at least one large link of size $\approx R_{\text{max}}$ which must be crossed in order for the population to reach the opposite edge of the system, and the time to cross this link sets the time scale to cross the system in the same way that the resistance of the largest link sets the scale of the resistance in the hopping conduction problem. Thus,

$$\langle \text{time to cross system of size } L_0 \rangle \approx \langle T(R_{\text{max}}, a) \rangle, \quad (38)$$

where $T(R_{\text{max}}, a)$ is given by (29) or (30) depending on the dimensionality of the system. This approximation should work better as κR_{max} increases, just as the estimate for the resistivity in (36) should work better as αR_{max} increases [48,52].

Now consider a very large system. The desired quantity is the mean infection time $\langle T_{\text{infection}}(L) \rangle$ —that is, the mean time for the population to travel between oases separated by some large distance $L \gg L_0$. This time is roughly equal to the mean FPT in the current parameter regime (that is, the limit of high growth rate on the oases). Because this time depends on the distance L —it is an extensive quantity—it is not analogous

to the resistivity in the semiconductor problem, which is an intensive quantity. It seems reasonable that, for large L , $\langle T_{\text{infection}}(L) \rangle \propto L$, but this should not be taken for granted. In order to show that this is the case and to arrive at an expression for $\langle T_{\text{infection}}(L) \rangle$, we will now employ some ideas from the theory of first passage percolation.

Consider the oasis system as consisting of nodes placed on a square ($d=2$) or cubic ($d=3$) lattice with lattice spacing L_0 with one large link of size R_{max} in between each node (we will ignore the time to cross the shorter links and the variations in the oasis configurations from one correlation-length-sized chunk to another); this is essentially the links-nodes-blobs picture of the system. The population starts at one node, and the desired quantity is the first passage time to some distant node located a distance L away along a lattice basis vector (or, equivalently, $n=L/L_0$ lattice points away). This is the basic problem of first passage percolation (FPP) [53]. One of the main results of FPP is that, as the separation between nodes $n \rightarrow \infty$, the FPT $\langle T(n) \rangle$ divided by n goes to a constant μ , conventionally called the time constant. Thus, the mean FPT rises linearly with distance between sites [with sublinear corrections of order $n^{1/2} \ln(n)$ [54]], indicating that the proper intensive quantity for the problem is the mean FPT divided by oasis separation. This is reassuring, as it reinforces the common-sense notion that $\langle T_{\text{infection}}(L) \rangle \propto L$ for large L . The value of μ depends on the underlying FPT probability distribution, but a general result is that $\mu \leq T_1$, where T_1 is the average time to cross one link [53]. For the case where the times are chosen from an exponential distribution, $\mu \approx 0.4T_1$ in two dimensions [55].

Since there is approximately one large link of size R_{max} in between each node, the time T_1 is given approximately by $\langle T(R_{\text{max}}, a) \rangle$. Furthermore, the distribution of times to cross the largest link is nearly exponential for large R_{max} [see (29) or (30)]; this suggests that the time constant for the oasis problem in $d=2$ should be of the order $0.4T_1$. The exact value is unimportant; the important fact is that the time constant is not too different from T_1 . Thus, to obtain a rough estimate of the infection time, one can simply use T_1 (the mean time to cross one large link) as an estimate for $\langle T_{\text{infection}} \rangle / n$. This gives the following:

$$\langle T_{\text{infection}}(L) \rangle \approx \frac{L}{L_0} \langle T(R_{\text{max}}, a) \rangle, \quad (39)$$

where $\langle T(R_{\text{max}}, a) \rangle$ is again given by (29) in $d=2$ and (30) in $d=3$ for large R , R_{max} is given by (34) and L_0 is given by (37).

Before continuing, it is probably good to stop at this point and briefly recall the approximations made to obtain the result quoted in (39): First, we have ignored the growth time on the grounds that it is small compared to the transit time between oases; second, we have simplified the picture of transport on the scale of L_0 , replacing the mess of oases with a single link of size R_{max} ; and third, we have used an upper limit on the time constant rather than the time constant itself. It should be noted that the first and second approximations tend to lead to underestimating $\langle T_{\text{infection}} \rangle$, while the third tends to lead to overestimating it. Finally, it should again be

stated that the infection time result quoted in (39) is meant to be an order-of-magnitude estimate.

C. Comparison with simulations

In order to confirm the predictions of the preceding section, we wrote a program capable of simulating a very large system in two dimensions. To make the simulation of such a large system tractable, we made some important simplifications which must be explained. The first of these is the most important: Rather than simulating the motion of individual particles, we simply assigned first passage times between oases. This allowed us to go to system sizes many orders of magnitude larger than we could have achieved via a full kinetic Monte Carlo simulation involving every particle.

The second simplification involves the nature of the FPT PDF used to generate the passage times between oases. The linear theory with a source produces an analytical expression for this FPT PDF [see (25) and Appendix B], but this is unwieldy and computationally expensive to calculate. However, for large R , the moments of this FPT PDF in $d=2$ approach those of an exponential distribution with parameter $gK_0(\kappa R)/K_0(\kappa a)$ [see (29)], where $\kappa \equiv \sqrt{z/D}$. Since it is the large- R separations which largely determine the infection time, we simply replaced the complicated FPT PDF between oases with this exponential distribution; the errors introduced by this simplification are serious only for small oasis separations, and these do not contribute much to the infection time.

The remaining simplifications are minor: We treated all the oases as points; we ignored the growth time, just as we have done in the analytical work presented in the preceding sections; and finally, we ignored the effects of neighboring oases on the first-passage time statistics between two oases. This final simplification again introduces errors mostly in areas of high oasis density where oasis separations are small. The bottlenecks of our particle current-carrying cluster occur where there are two oases separated by a large region of desert, and in these areas the FPT statistics should be close to those derived in the case of two oases in an infinite desert.

Before presenting our simulation results, we must first provide some details of the way time was scaled in our simulations. We measured time in units of the average time needed to cross a link of size R_{max} ; that is, we used the FPT PDF

$$f_N(R, \tau) = \frac{K_0(\kappa R)}{K_0(\kappa R_{\text{max}})} \exp\left(-\frac{K_0(\kappa R)}{K_0(\kappa R_{\text{max}})} \tau\right) \quad (40)$$

to generate times between oases separated by a distance R . There is one further approximation that we made in our simulations simply for the sake of convenience: We used the large-argument asymptotic form for $K_0(x)$ of $\sqrt{\pi/2x}e^{-x}$. Like some of the other simplifications and approximations we made in the simulations, this approximation is not good for small oasis separations, but the errors introduced are ultimately unimportant given the contribution of the small oasis jumps to the transit time.

If our theory is correct, the mean time to cross one block of size L_0 in these units (in units of τ) should be of order 1,

and the mean infection time should be $\approx L/L_0$. If κ and R_{\max} are adjusted in such a way so that their product remains constant, then this amounts to a trivial rescaling of space, and $\tau_{\text{infection}}$ should simply vary as $1/R_{\max}$. This is already captured through the dependence of $\tau_{\text{infection}}(L)$ on L_0 , and so we can write

$$\langle \tau_{\text{infection}}(L) \rangle = \left(\frac{L}{L_0} \right) F(\kappa R_{\max}), \quad (41)$$

where $F(\kappa R_{\max})$ is some function of order unity. We thus expect that a graph of $\langle \tau_{\text{infection}} \rangle$ versus L/L_0 for large L should be a straight line with slope of order 1 the exact value of which should only depend on the product κR_{\max} .

For each simulation run, κ and the oasis density n were input, R_{\max} and L_0 were calculated from (34) and (37), respectively, and a starting oasis was chosen near the center of the system. The simulation then proceeded one infection event at a time, with infection times between oases generated using the distribution given in (40). In order to speed up the simulation, we set a maximum distance R_{cut} beyond which oases were effectively disconnected. This allowed us to generate new oases “on-the-fly” as the simulation proceeded; together with our practice of throwing away information about an oasis once it was reached, this allowed us to only keep a small subset of oases in memory at any one time, thus allowing for the simulation of very large systems. The value of R_{cut} was chosen so as to make the probability of a missed event—that is, a jump event of size larger than R_{cut} occurring over the course of the simulation—very small ($<10^{-3}$).

In early simulation runs, we found that our starting oasis would sometimes be isolated from the rest of the cluster, leading to larger-than-expected infection times with a large contribution from the time for the population to make the first jump. In the limit as $L \rightarrow \infty$ —the large-distance limit we are interested in—this contribution to the infection time, which does not grow with L , should become negligible, but for finite values of L it can be important. In order to eliminate this effect from our simulations without going to system sizes too large to be simulated in a reasonable amount of time, we allowed the population to “find” the cluster: We restarted the simulation once an oasis at least $2R_{\max}$ from the starting oasis had been hit with the newly hit oasis as the new starting oasis. The choice of $2R_{\max}$ is admittedly arbitrary, but it did serve to eliminate the undesired effect from our simulations.

Once the population was restarted, the simulation continued one oasis infection event at a time. When an oasis within a small distance $\delta \ll L_0$ of one of a set of concentric rings centered at the starting oasis was hit, the time and distance from the starting oasis were recorded; once all oases in some final ring were infected, the simulation ended. The results of the simulation are shown in Fig. 5. The data confirms our picture of transport: The slopes of the best-fit lines through the data are indeed of order 1, suggesting that R_{\max} is the correct length scale of the largest jumps the population must make on its way through the system and that L_0 is the correct length scale for the distance between these large jumps (of course, the population left behind the front edge will eventually make larger jumps to infect isolated oases, but this is

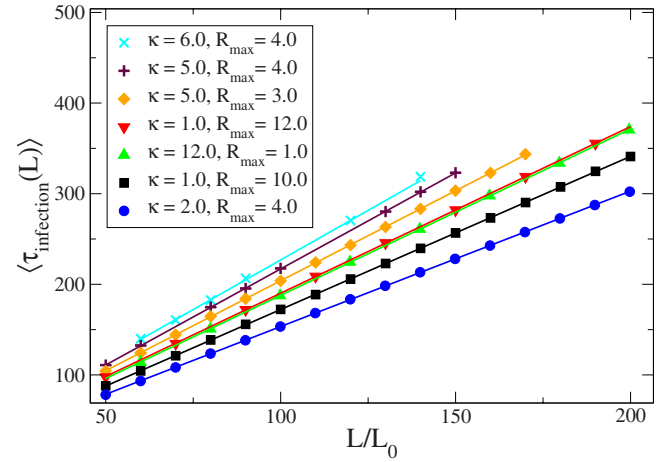


FIG. 5. (Color online) First passage times across a large system shown for seven different combinations of κ and R_{\max} . Error bars are not shown since they are, in most cases, smaller than the symbol size. The lines represent best-fit lines for each κ , R_{\max} . The two lines with $\kappa R_{\max} = 12.0$ lie nearly on top of one another, as one would expect; we have omitted every other data point for each of these runs for clarity. Note that the value of the slope [which is equal to $F(\kappa R_{\max})$] increases as κR_{\max} increases.

unimportant in trying to determine the infection time). Note that there are some “missing” points on the two lines with the highest κR_{\max} . This is due to the presence of oases inside those rings which were not hit before the simulation time ended. As κR_{\max} is increased, such outlying oases take longer to hit, but since their “extra” contribution to the mean transit time does not scale with L , they do not affect our $L \rightarrow \infty$ results.

The slope for each line is equal to the scaling function $F(\kappa R_{\max})$ for those values of κ and R_{\max} ; note that $F(\kappa R_{\max})$ appears to increase for increasing values of κR_{\max} . This is likely due to that fact that, as κR_{\max} increases, the correlation length L_0 increases, and thus the number of smaller oasis separations between the large oasis separations increases as well. However, the important point is that the slopes are all of order 1.

V. CONCLUSIONS, REMARKS, AND FUTURE WORK

In this paper, we have examined transport in a reaction-diffusion model with disorder in the reaction rates. Such models have been used in the past to study bacterial population dynamics and the movement of plankton in the oceans. Our model consists of particles which are allowed to diffuse with diffusion constant D and compete for resources ($2A \rightarrow A$) everywhere with rate b , but which can only give birth ($A \rightarrow 2A$) on small patches called oases at rate y and which die ($A \rightarrow 0$) everywhere else at rate z . We have considered the limit in which the growth rate on the oases is very high and the oasis density is very low; in this limit, the time needed for a small population to grow on an oasis is much smaller than the typical time needed to jump from oasis to oasis, and thus transport can be thought of as a first passage process. Because the population density traveling from one

oasis to another is small, it is necessary to consider discreteness effects. In order to determine the first passage time probability density function (FPT PDF) between two oases, we have employed a simplified model in which competition is ignored and the initially infected oasis is replaced by a particle source. Simulations suggest that this model correctly predicts the FPT PDF for large oasis separations.

We have used an analogy with the theory of hopping conduction to argue that the largest oasis separations in the particle current-carrying cluster largely determine the time taken for a population to travel to a given target. The scale of these separations can be found using continuum percolation theory, as in the hopping conduction problem. There is a significant difference between the two problems: Ours is dynamic, while the hopping conduction problem is not. However, the use of results from first passage percolation theory suggest that the time scale for transit should still be determined by the largest oasis separations in the relevant particle current-carrying cluster.

There are certainly many future areas of study related to our work. First, there is the obvious question of what happens when the oases are not identical, but instead have their sizes and growth rates picked from some distribution. One might hope that the theory of variable-range hopping [46] would be useful in this case, though it remains to be seen whether the dynamic nature of the problem would make a fruitful mapping possible. There is also the problem of extinction: What happens when the oases are allowed to die out at some rate? We believe that the active to absorbing state transition that would occur as the oasis death rate is raised should be the same as that found in the contact process with disorder [21,23–25], but simulations are needed to confirm this.

ACKNOWLEDGMENTS

We would like to thank Bryan Clark, John Gergely, David Nelson, Mark Rudner, Nadav Shnerb, Richard Sowers, and Uwe Täuber for helpful discussions. This work was supported in part by NSF-DMR Grant Nos. 03-14279 and 03-25939 (ITR) (UIUC Materials Computation Center), and by the L.S. Edelheit Family Endowed Fund in Biological Physics. We gratefully acknowledge the use of the Turing cluster, which is maintained and operated by the Computational Science and Engineering Program at the University of Illinois [56].

APPENDIX A: DERIVATION OF THE FORMULA FOR y_c

The cutoff value of the growth rate y below which a population placed on an oasis will die out as $t \rightarrow \infty$ can be estimated using the mean-field equation (1) with $b=0$. For values of y greater than the cutoff, the population will continue to increase without limit as $t \rightarrow \infty$; for $y < y_c$, the population will eventually die out. At y_c , there will be a steady-state solution. Hence, one way of finding the cutoff is to try to match solutions to the steady-state equation for $|x| < a$ and $|x| > a$ at $|x|=a$ (the edge of the oasis). Only along a certain line in parameter space will this be possible.

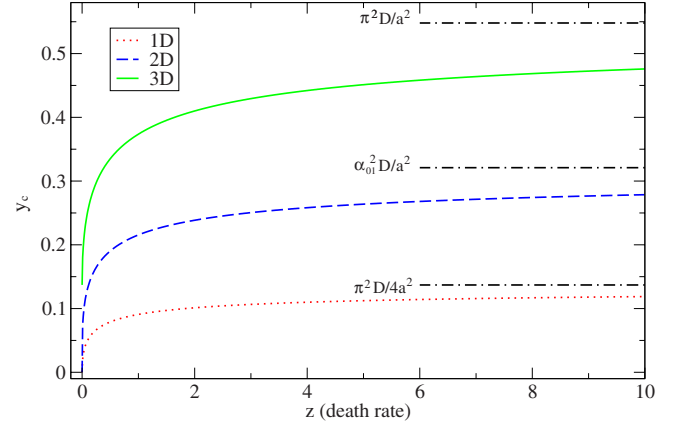


FIG. 6. (Color online) Cutoff growth rate y_c as a function of death rate z with $a=3.0$, $D=0.5$. Here α_{01} is the first zero of J_0 . Note that in one and two dimensions, an arbitrarily small growth rate with $z=0$ will allow a stable population to take hold; in three dimensions, $y_c(z=0) = \pi^2 D / 4a^2$.

In one dimension, the steady-state mean-field equation with $b=0$ is solved by $c(0)\cos(\sqrt{y/D}x)$ for $|x| < a$ and $c(a)e^{-\kappa(|x|-a)}$ for $|x| > a$. Matching the functions and derivatives at $|x|=a$ leads to

$$y_c = z \cot^2\left(\sqrt{\frac{y_c}{D}}a\right) \quad (1D), \quad (A1)$$

which is precisely (6). In two dimensions, a similar calculation leads to

$$y_c = z \left(\frac{J_0\left(\sqrt{\frac{y_c}{D}}a\right)K_1(\kappa a)}{J_1\left(\sqrt{\frac{y_c}{D}}a\right)K_0(\kappa a)} \right)^2, \quad (2D) \quad (A2)$$

while in three dimensions we have obtained

$$y_c = z \tan^2\left(\pi - \sqrt{\frac{y_c}{D}}a\right) \quad (3D). \quad (A3)$$

These equations can be solved numerically to determine y_c . A plot of y_c as a function of z in one, two, and three dimensions, with all other parameters fixed, is shown in Fig. 6. Note that y_c only has meaning in the mean-field limit; taking fluctuations into account leads to the conclusion that single isolated oasis will die out with probability 1 as $t \rightarrow \infty$.

APPENDIX B: ASYMPTOTIC ANALYSIS OF THE MOMENTS OF $f_N(x, t)$

In this appendix, we derive the results for the asymptotic moments of $f_N(x, t)$ quoted in (26), (29), and (30); the lattice result (33) can be obtained in a similar manner. In any dimension, $P_{\text{none}}(R, a, t) \approx \exp[-gY(R, a, t)]$, where $Y(R, a, t)$ is given by

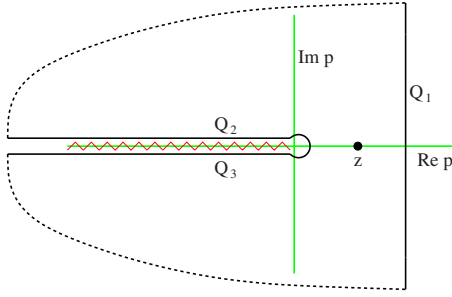


FIG. 7. (Color online) Schematic of the contour integral which must be done to find $Y(R, a, t)$. The dashed lines represent contributions to the integral that vanish as they are moved further from the origin.

$$Y(R, a, t) = \frac{(a/R)^{d/2-1}}{2\pi i} \int_{\mathcal{L}} ds \frac{e^{st} K_{d/2-1} \left(\sqrt{\frac{s+z}{D}} R \right)}{K_{d/2-1} \left(\sqrt{\frac{s+z}{D}} a \right)}. \quad (\text{B1})$$

Although in $d=1$ and $d=3$ this Laplace transform machinery is unnecessary—we can simply perform the integral over time appearing in (19)—it is easier to determine the asymptotic behavior of the moments of $f_N(R, a, t)$ in all dimensions by using these tools. Changing variables to $p=s+z$ leads to $Y(R, a, t) = [(a/R)^{d/2-1} e^{-zt} / (2\pi i)] Q_1(R, a, t)$, where

$$Q_1(R, a, t) = \int_{\mathcal{L}} dp \frac{e^{pt} K_{d/2-1} \left(\sqrt{\frac{p}{D}} R \right)}{(p-z)^2 K_{d/2-1} \left(\sqrt{\frac{p}{D}} a \right)}. \quad (\text{B2})$$

This integral can be evaluated using contour integral techniques. There is one second-order pole at $p=z$ and a branch cut which we will take to lie on the real p axis from $p=0$ to $p=-\infty$. Our contour will be taken to enclose the pole at $p=z$, and consists of three parts: Q_1 , the value of which we wish to find; and Q_2 and Q_3 , whose values must add with that of Q_1 to equal $2\pi i \Xi$, where Ξ is the residue at $p=z$. The space is shown schematically in Fig. 7. Using the residue theorem and changing integration variables to $u=-p$ gives

$$Q_1(R, a, t) = 2\pi i t e^{zt} \frac{K_{\mu}(\kappa R)}{K_{\mu}(\kappa a)} - 2\pi i \frac{e^{zt} R K_{\mu+1}(\kappa R) K_{\mu}(\kappa a)}{\sqrt{4Dz} [K_{\mu}(\kappa a)]^2} + 2\pi i \frac{e^{zt} a K_{\mu}(\kappa R) K_{\mu+1}(\kappa a)}{\sqrt{4Dz} [K_{\mu}(\kappa a)]^2} - \int_0^{\infty} du \frac{e^{-tu}}{(u+z)^2} \frac{M_{\mu}(R, a, u)}{K_{\mu} \left(\iota \sqrt{\frac{u}{D}} a \right) K_{\mu} \left(-\iota \sqrt{\frac{u}{D}} a \right)}, \quad (\text{B3})$$

where we have used $\mu=d/2-1$ and $M_{\mu}(R, a, u) = 2i \text{Im}[K_{\mu}(\iota \sqrt{\frac{u}{D}} R) K_{\mu}(-\iota \sqrt{\frac{u}{D}} a)]$. We see that $Y(R, a, t)$ thus has the form $C_1 t - C_2 + C_3 h(t)$, where the C_n are constants in time and $h(t)$ is given by some complicated integral. Since $Y(R, a, 0) = 0$, we can let $C_3 = C_2$ and $h(0) = 1$. It should be clear that $h(\infty) = 0$, and that $h(t) \leq 1$ for all t . This is enough to prove the asymptotic results for the moments of $f_N(R, a, t)$ quoted in Sec. III C. These moments are given by $\langle T^j(R, a) \rangle = j \int_0^{\infty} dt P_{\text{none}}(R, a, t) t^{j-1}$; plugging in the form for $Y(R, a, t)$ gives

$$\langle T^j(R, a) \rangle = j \int_0^{\infty} dt e^{-g\{C_1 t - C_2[1-h(t)]\}} t^{j-1}. \quad (\text{B4})$$

The constant C_2 goes to 0 as $R \rightarrow \infty$, so one can Taylor expand $\exp\{gC_2[1-h(t)]\}$ and arrive at

$$\langle T^j(R, a) \rangle = j \int_0^{\infty} dt e^{-gC_1 t} t^{j-1} \{1 + gC_2[1-h(t)] + \dots\}. \quad (\text{B5})$$

Keeping only the lowest order term, we get $\langle T^j(R, a) \rangle = j!(gC_1)^{-j}$ as $R \rightarrow \infty$. Looking at (B3), we see that $C_1 = (a/R)^{d/2-1} K_{d/2-1}(\kappa R) / K_{d/2-1}(\kappa a)$. We are now ready to plug in the functional forms for $K_{d/2-1}$ and arrive at the final asymptotic expressions for $\langle T^j(R, a) \rangle$,

$$\langle T^j(x) \rangle = j! \frac{e^{\kappa|x|j}}{g^j} \quad (\text{1D}),$$

$$\langle T^j(R, a) \rangle = j! \left[\frac{K_0(\kappa a)}{g K_0(\kappa R)} \right]^j \quad (\text{2D}),$$

$$\langle T^j(R, a) \rangle = j! \left(\frac{R}{a} \right)^j \frac{e^{\kappa(R-a)j}}{g^j} \quad (\text{3D}), \quad (\text{B6})$$

where $|x| = R - a$ (the distance from the origin to the edge of the oasis nearest the origin).

- [1] R. Kroon, H. Fleurent, and R. Sprik, Phys. Rev. E **47**, 2462 (1993).
 [2] J. D. Murray, *Mathematical Biology* (Springer-Verlag, New York, 1993).
 [3] D. R. Nelson and N. M. Shnerb, Phys. Rev. E **58**, 1383 (1998).
 [4] K. A. Dahmen, D. R. Nelson, and N. M. Shnerb, e-print arXiv:cond-mat/9903276v1.

- [5] K. A. Dahmen, D. R. Nelson, and N. M. Shnerb, J. Math. Biol. **41**, 1 (2000).
 [6] M. Mimura, H. Sakaguchi, and M. Matsushita, Physica A **282**, 283 (2000).
 [7] K. M. Page, N. A. M. Monk, and P. K. Maini, Phys. Rev. E **76**, 011902 (2007).
 [8] J. von Hardenberg, E. Meron, M. Shachak, and Y. Zarmi, Phys.

- Rev. Lett. **87**, 198101 (2001).
- [9] D. A. Birch, Y. K. Tsang, and W. R. Young, Phys. Rev. E **75**, 066304 (2007).
- [10] P. Grassberger and A. de la Torre, Ann. Phys. **122**, 373 (1979).
- [11] H. Janssen, Z. Phys. B: Condens. Matter **42**, 151 (1981).
- [12] H. Hinrichsen, Adv. Phys. **49**, 815 (2000).
- [13] H. Janssen and U. Täuber, Ann. Phys. **315**, 147 (2005).
- [14] U. Täuber, M. Howard, and B. P. Vollmayr-Lee, J. Phys. A **38**, R79 (2005).
- [15] J. M. Debierre and R. M. Bradley, Phys. Rev. E **50**, 2467 (1994).
- [16] R. Dickman and M. A. Muñoz, Phys. Rev. E **62**, 7632 (2000).
- [17] E. Moro, Phys. Rev. Lett. **87**, 238303 (2001).
- [18] D. Panja, Phys. Rep. **393**, 87 (2004).
- [19] N. G. van Kampen, *Stochastic Processes in Physics and Chemistry* (Elsevier Science, Amsterdam, The Netherlands, 2007).
- [20] H. K. Janssen, Phys. Rev. E **55**, 6253 (1997).
- [21] A. G. Moreira and R. Dickman, Phys. Rev. E **54**, R3090 (1996).
- [22] I. Webman, Philos. Mag. B **77**, 1401 (1998).
- [23] G. Szabó, H. Gergely, and B. Oborny, Phys. Rev. E **65**, 066111 (2002).
- [24] T. Vojta and M. Y. Lee, Phys. Rev. Lett. **96**, 035701 (2006).
- [25] T. Vojta, A. Farquhar, and J. Mast, Phys. Rev. E **79**, 011111 (2009).
- [26] J. Hooyberghs, F. Iglói, and C. Vanderzande, Phys. Rev. Lett. **90**, 100601 (2003).
- [27] J. Hooyberghs, F. Iglói, and C. Vanderzande, Phys. Rev. E **69**, 066140 (2004).
- [28] A. Lemarchand, A. Lesne, and M. Mareschal, Phys. Rev. E **51**, 4457 (1995).
- [29] G. Grinstein, M. A. Muñoz, and Y. Tu, Phys. Rev. Lett. **76**, 4376 (1996).
- [30] J. Armero, J. M. Sancho, J. Casademunt, A. M. Lacasta, L. Ramírez-Piscina, and F. Sagués, Phys. Rev. Lett. **76**, 3045 (1996).
- [31] J. Armero, J. Casademunt, L. Ramírez-Piscina, and J. M. Sancho, Phys. Rev. E **58**, 5494 (1998).
- [32] V. Méndez, J. Fort, H. G. Rotstein, and S. Fedotov, Phys. Rev. E **68**, 041105 (2003).
- [33] M. A. Santos and J. M. Sancho, Phys. Rev. E **59**, 98 (1999).
- [34] F. Sagués, J. M. Sancho, and J. García-Ojalvo, Rev. Mod. Phys. **79**, 829 (2007).
- [35] G. Ódor, Rev. Mod. Phys. **76**, 663 (2004).
- [36] A. R. Missel and K. A. Dahmen, Phys. Rev. Lett. **100**, 058301 (2008).
- [37] J. Joo and J. L. Lebowitz, Phys. Rev. E **72**, 036112 (2005).
- [38] A. L. Lin, B. A. Mann, G. Torres-Oviedo, B. Lincoln, J. Kas, and H. L. Swinney, Biophys. J. **87**, 75 (2004).
- [39] M. Assaf and B. Meerson, Phys. Rev. E **75**, 031122 (2007).
- [40] There is a subtle but ultimately unimportant inconsistency here: We have heretofore implicitly assumed that the creation process $0 \rightarrow A$, at the source is a Poisson process with rate g , but now we are taking it to be a process in which N particles are released at regular intervals Δt . However, since the time scales of interest in the problem are $\gg 1/g$, this discrepancy is insignificant.
- [41] S. Redner, *A Guide to First-Passage Processes* (Cambridge University Press, Cambridge, UK, 2001).
- [42] M. Abramowitz and I. A. Stegun, *Handbook of Mathematical Functions with Formulas, Graphs, and Mathematical Tables* (Dover, New York, 1964).
- [43] A. Donev, e-print arXiv:cs/0703096v2.
- [44] P. Grassberger and I. Procaccia, Phys. Rev. A **26**, 3686 (1982).
- [45] S. Redner and K. Kang, Phys. Rev. A **30**, 3362 (1984).
- [46] B. I. Shklovskii and A. L. Efros, *Electronic Properties of Doped Semiconductors* (Springer-Verlag, Berlin, 1984).
- [47] V. Ambegaokar, B. I. Halperin, and J. S. Langer, Phys. Rev. B **4**, 2612 (1971).
- [48] J. Kurkijärvi, Phys. Rev. B **9**, 770 (1974).
- [49] D. Stauffer and A. Aharony, *Introduction to Percolation Theory* (Routledge, London, 1994).
- [50] According to Hunt and others [51], there exists another length scale l , which, together with L_0 , characterizes the structure of the cluster in $d=3$. This length scale is associated with the distance between large links along the direction of current motion.
- [51] A. Hunt, *Percolation Theory for Flow in Porous Media* (Springer-Verlag, Berlin, 2005).
- [52] V. Ambegaokar, S. Cochran, and J. Kurkijärvi, Phys. Rev. B **8**, 3682 (1973).
- [53] H. Kesten, Lect. Notes Math. **1180**, 125 (1986).
- [54] K. Alexander, Ann. Appl. Probab. **3**, 81 (1993).
- [55] S. Alm and R. Parviainen, Combinatorics, Probab. Comput. **11**, 433 (2002).
- [56] Turing is a 1536-processor Apple G5 X-serve cluster devoted to high performance computing in engineering and science.